ORGANOMETALLICS

Article

Cite This: *Organometallics* 2018, 37, 1358−1367

Chain-Walking Polymerization of Linear Internal Octenes Catalyzed by α-Diimine Nickel Complexes

Fuzhou Wang,*[,†,‡] Ryo Tanaka,[‡] Qingshan Li,[§] Yuushou Nakayama,[‡] and Takeshi Shiono*[,‡]

[†]Institute of Physical Science and Information Technology, Anhui University, Hefei, Anhui 230601, China

[‡]Graduate School of Engineering, Hiroshima University, Kagamiyama 1-4-1, Higashi-Hiroshima 739-8527, Japan

[§]Department of Chemistry, Nankai University, Tianjin 300071, China

Supporting Information

ABSTRACT: The chain-walking polymerization of linear internal alkenes (i.e., *trans*-2-, 3-, and 4-octenes) using α-diimine nickel catalysts activated with modified methylaluminoxane (MMAO) was studied in comparison with the corresponding terminal alkene polymerization. The rates of polymerization were found to decrease in the following order: 1-octene > 4-octene ≥ 2-octene ≫ 3-octene. The obtained branched poly(2-octene)s and poly(4-octene)s with high molecular weight and M_w/M_n less than 2 were amorphous polymers with low glass transition temperature (T_g) of approximately −66 °C. At 0 °C, 4-octene polymerized in a living/controlled manner. The NMR analyses of the polymers showed that the chain-walking polymerization of 4-octene gave periodically branched polymers with the constant branching density, while that of 2-octene gave the polymer possessing fewer branches than the expected value due to monomer-isomerization. The (*n*+2),(*n*+3)- and (*n*+3),(*n*+2)-insertions of the internal (*n*+2)-alkene [$CH_3(CH_2)_nCH{=}CH(CH_2)_mCH_3$] followed by chain-walking were confirmed by the ^{13}C NMR analysis of the produced polymers.

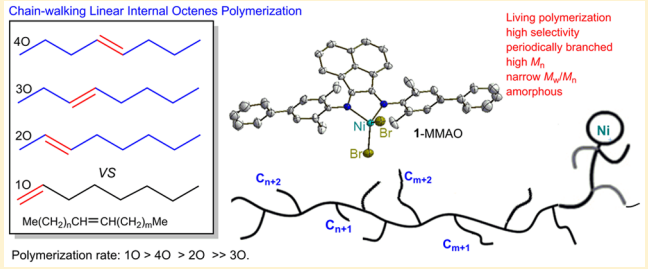

INTRODUCTION

The research of ethylene and 1-alkene polymerizations catalyzed by late-transition-metal complexes[1] is a great highlight for the development of novel polyolefin materials in recent years.[2] Nickel and palladium catalysts[3,4] ligated by α-diimine showed good activities for ethylene and 1-alkene polymerizations to produce a variety of branched polyolefins because of their chain-walking feature.[5] The branching degree of the polymer can be controlled by polymerization conditions and the catalyst structures.[6,7]

Chain-branching formation in linear 1-alkene polymerization[7] with α-diimine nickel and palladium catalysts is shown in Scheme 1. The mechanism involves 1,2- and 2,1-insertion followed by chain-walking,[7] in which the active metal center undergoes chain-walking to the terminal carbon followed by monomer insertion. 1,2-Insertion gives methyl branch (ii) in a 2,ω-enchainment, while 2,1-insertion gives a long methylene sequence (iii) in a 1,ω-enchainment (chain-straightening).[8] If the metal fails to chain walk after 1,2-insertion, the final polymer contains *n*-alkyl ($C_{\omega-2}$) branches (i) found in common poly(1-alkene)s. The highly branched polymers with methyl and *n*-alkyl groups are amorphous, while the chain-straightened polymers are semicrystalline.[7b]

The amount and type of branching are dependent on the catalyst structure and polymerization conditions,[9] which in turn strongly influence the polymer crystallinity.[1d] For example, Chen et al. reported that a series of iminopyridyl nickel catalysts containing both the dibenzhydryl and the naphthyl moieties polymerized ethylene with high activity and high thermal stability,[10] and they generated semicrystalline poly(1-alkene)s with high melting temperatures. Coates et al. reported precision chain-walking polymerization of linear 1-alkenes using the "sandwich" α-diimine nickel catalysts, which afforded semicrystalline "polyethylene".[7b] α-Diimine nickel complexes were reported to catalyze polymerization of 2-butene[11] and 2-pentene[12] to afford high-molecular-weight polymers. However, the chain-walking polymerization of higher 2-, 3-, and 4-alkenes with nickel and palladium catalysts have been reported only in a limited number of cases.

We have previously reported a series of phenyl substituted α-diimine nickel complexes[13] activated by Et_2AlCl or MMAO exhibited high activities toward ethylene polymerization to afford highly branched polyethylene, and we conducted 1-alkene polymerization[14] to afford branched polymers with high molecular weight. Recently, we synthesized and characterized a series of high molecular weight poly(2-alkene) by a phenyl substituted α-diimine nickel complex,[15] and these 2-alkenes were polymerized in a living manner to produce amorphous polymers at 0 °C. We also reported the first polymerization of *trans*-4-octene with α-diimine nickel catalysts bearing *ortho*-*sec*-phenethyl groups at low temperature to obtain periodically propyl-branched polymethylene (i.e., poly(1-propylpentan-1,5-diyl)).[16] In this context, we became very interested in the

Received: January 22, 2018
Published: April 26, 2018

DOI: 10.1021/acs.organomet.8b00042
Organometallics 2018, 37, 1358−1367

Scheme 1. Chain-walking mechanism for linear 1-alkene polymerization by α-diimine nickel and palladium catalysts

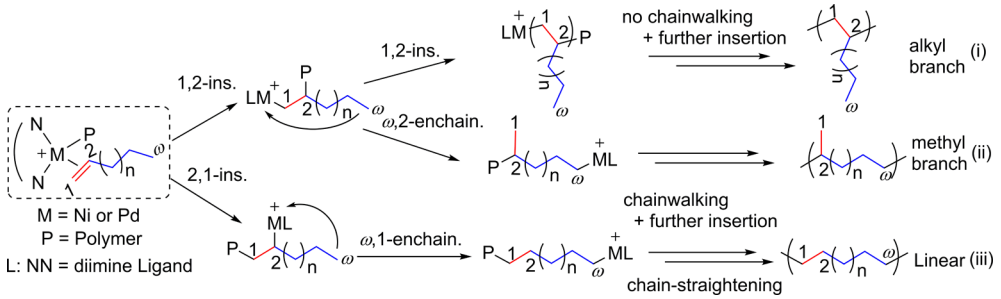

polymerization of linear internal octenes (i.e., 2-, 3-, and 4-octenes). This work extends our previous studies on 2-octene[15] and 4-octene[16] polymerizations and gives a whole mechanism on the chain-walking polymerization of linear internal alkenes. The effects of catalyst structure, polymerization temperature, [Al]/[Ni] molar ratio, and linear octene isomers type on productivity, selectivity of monomer insertion, and polymer structure/properties (i.e., total branching, branch-type and thermal behavior) are investigated.

RESULTS AND DISCUSSION

Synthesis and Characterization. α-Diimine nickel precatalysts used in this study are summarized in Scheme 2. Complexes **1**, **3**, **5**, and **6** were previously reported.[14,17] Complexes **2** and **4** were synthesized in this study from the corresponding ligand and $(DME)NiBr_2$[18] in high yields.

Scheme 2. Synthesis of α-Diimine Nickel Complexes 1−6

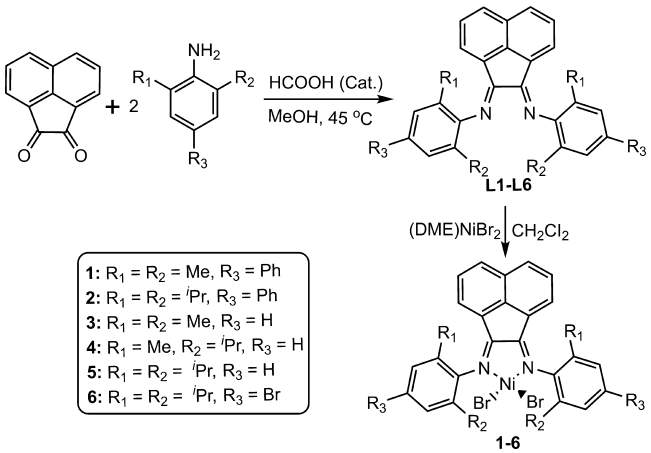

Suitable crystal of complex **2** for X-ray diffraction were obtained at room temperature by double layering a CH_2Cl_2 solution of the complex with *n*-hexane. The molecular structure of **2** was confirmed by single-crystal X-ray diffraction and the corresponding ORTEP diagram is shown in Figure 1. Crystal data, data collection, and refinement parameters are listed in Table S1 (see the Supporting Information). The molecular structure of complex **1**[14] was reported in our recent publication (Figure S9).

The X-ray structure analysis indicates that complex **2** has a pseudo-tetrahedral geometry about the Ni center, showing C_{2v} molecular symmetry. In solid state, complex **2** clearly shows the *N,N*-chelating bis(imino)acenaphthene structure with a phenyl group connected in the *para*-aryl position. The two isopropyl in the 2,6-position of the aniline fragments in complex **2** located

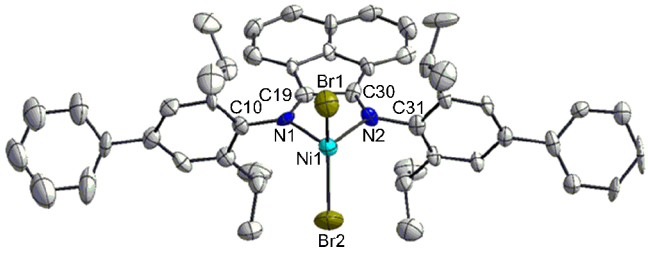

Figure 1. Molecular structure of the catalyst precursor **2** with 50% probability level, and H atoms have been omitted for clarity. Selected bond lengths (Å) and angles (deg) for complexes: Br1−Ni1, 2.333(3); Br2−Ni1, 2.299(3); Ni1−N1, 2.041(11); Ni1−N2, 1.992(11); N1−C10, 1.436(17); N1−C19, 1.248(16); Br1−Ni1−Br2, 125.83(12); N1−Ni1−N2, 81.0(5); N1−Ni1−Br2, 115.1(3); N2−Ni1−Br2, 116.7(4); C10−N1−C19, 119.6(12).

above and below the Ni1 coordinative geometry plane (Figure 1). The two aryl rings of the α-diimines lie nearly perpendicular to the plane formed by the nickel and coordinated nitrogen atoms. The N1−Ni1−N2 bite angle in complex **2** is 81.0(5)° and highlights the distortion imposed by the chelating ligand on the geometry. The Br1−Ni1−Br2 angle is 125.83(12)°. The two imino C═N bonds have typical double bond character with C19═N1 bond lengths of 1.248 (16) Å. The molecular structures of complexes **1** and **2** are very similar (Figure S9).[14] In fact, the Ni−N bond distances in **2** (2.041(11) and 1.992(11) Å) are similar to those determined for complex **1** (2.041(5) Å), and the Ni−Br bond distances in complexes **1** and **2** are almost identical (2.333(3) and 2.299(3) Å for **2** vs 2.3343(12) Å for **1**). In addition, the N−Ni−Br angles of complex **2** (115.1(3) and 116.7(4)°) also approximate to those of complex **1** (112.96(6)°). These *para*-phenyl substituted α-diimine nickel complexes may induce a conjugation effect in olefin polymerization.[14]

Polymerization of Linear Octene isomers. All the catalyst precursors **1**−**6** were applied to *trans*-4-octene (4O) polymerization at room temperature (20 °C) using MMAO as a cocatalyst. The initial results are summarized in Table 1.

First, polymerization of 4O was investigated by **1**-MMAO at 20 °C with the [Al]/[Ni] molar ratio from 300 to 700 (entries 1−3, Table 1). The catalytic activity of complex **1** did not significantly depend on the [Al]/[Ni] ratio and the maximum catalytic activity was observed with the [Al]/[Ni] ratio of 500 (entry 3). Besides, the highest molecular weight (M_n = 46.7 kg mol^{-1}) of the product was also observed with the [Al]/[Ni] ratio of 500 (entry 2).

Then, the effect of catalyst precursors **1**−**6** was investigated with [Al]/[Ni] ratio of 500 at 20 °C (entries 2 and 4−8, Table 1). All complexes **1**−**6** produced polymers in moderate yields with high molecular weight ($M_n \geq$ 18.7 kg mol^{-1}) and narrow

DOI: 10.1021/acs.organomet.8b00042
Organometallics 2018, 37, 1358−1367

Table 1. Polymerization of *trans*-4-Octene (4O) Catalyzed with 1−6 Activated by MMAO[a]

entry	complex	R_1	R_2	R_3	[Al]/[Ni]	yield (mg)	activity[b]	M_n[c] (kg mol^{-1})	M_w/M_n[c]	N[d] (μmol)	branches[e] /1000C
1	**1**	Me	Me	Ph	300	268	13.4	31.9	1.49	8.4	125
2	**1**				500	346	17.3	46.7	1.55	7.4	125
3	**1**				700	297	14.8	44.1	1.94	6.7	125
4	**2**	^{i}Pr	^{i}Pr	Ph	500	302	15.1	49.0	1.52	6.2	125
5	**3**	Me	Me	H	500	205	10.3	20.7	1.46	9.9	125
6	**4**	Me	^{i}Pr	H	500	199	10.0	22.9	1.89	8.7	125
7	**5**	^{i}Pr	^{i}Pr	H	500	181	9.1	27.9	1.49	6.5	125
8	**6**	^{i}Pr	^{i}Pr	Br	500	195	9.8	33.2	1.85	5.9	125

[a]Polymerization conditions: Ni = 10 μmol; cocatalyst MMAO; 0.5 g of *trans*-4-octene; polymerization time, 2 h; temperature, RT ≈ 20 °C; solvent, toluene; total volume, 5 mL. [b]In unit of kg (mol Ni h)$^{-1}$. [c]Determined by GPC relative to polystyrene standards. [d]Number of polymer chains calculated by yield and M_n. [e]Branching numbers per 1000 carbon atoms were determined by ^{1}H NMR spectroscopy.

Table 2. Polymerization of 1-Octene (1O), *trans*-2-Octene (2O), *trans*-3-Octene (3O), and *trans*-4-Octene (4O) with 1-MMAO[a]

entry	monomer	temp (°C)	time (h)	yield (mg)	activity[b]	M_n[c] (kg mol^{-1})	M_w/M_n[c]	N[d] (μmol)	branches[e] /1000 C
1	4O	−25	2	106	5.3	30.3	1.25	3.5	125
2	4O	0	2	207	10.4	53.8	1.19	3.8	125
3	4O	25	2	338	16.9	45.1	1.33	7.5	125
4	4O	50	2	253	12.6	34.7	1.64	7.3	125
5	4O	75	2	90	4.5	13.3	1.72	6.8	125
6	4O	0	0.5	57	11.4	16.1	1.14	3.5	125
7	4O	0	1	110	11.0	28.5	1.15	3.9	125
8	4O	0	4	325	8.1	83.4	1.20	3.9	125
9	4O	25	4	434	10.9	73.4	1.42	5.9	125
10	3O	0	2	trace					
11	3O	25	2	trace					
12	2O	0	2	182	9.1	25.5	1.11	7.1	121
13	2O	25	2	235	11.8	46.8	1.63	5.0	119
14	1O	0	2	324	16.2	89.0	1.08	3.6	100
15	1O	25	2	456	22.8	132.6	1.31	3.4	86

[a]Polymerization conditions: Ni = 10 μmol; cocatalyst MMAO, [Al]/[Ni] = 500; 0.5 g of *trans*-octene; solvent, toluene; total volume, 5 mL. [b]In unit of kg (mol Ni·h)$^{-1}$. [c]Determined by GPC relative to polystyrene standards. [d]Number of polymer chains calculated by yield and M_n. [e]Branching numbers per 1000 carbon atoms were determined by ^{1}H NMR spectroscopy.

molecular weight distribution (M_w/M_n = 1.40−1.94). The activities decreased in the following order, **1** ≥ **2** ≥ **3** ≥ **4** ≥ **6** ≥ **5**. The molecular weight of the polymers decreased in the following order, **2** ≥ **1** ≥ **6** ≥ **5** ≥ **4** ≥ **3**.

Electronic effect of the ligands can be discussed by comparing nickel complexes **2**, **5**, and **6** (entries 4, 7, and 8). The results indicate that the nickel complexes with electron-withdrawing groups [**2**(Ph) > **6**(Br) > **5**(H)] in the *para*-aryl position showed higher catalytic activity for 4O polymerization and gave the polymer with higher molecular weight.[14,15] Complex **1** bearing a phenyl group in the *para*-aryl position also exhibited higher activity than the corresponding nonsubstituted complex **3** (entries 4 vs 7, Table 1)

Steric effect of *ortho*-position in anilinic moiety can be evaluated by comparing **1** to **2** and **3** to **5** (entries 2, 4, 5, and 7). The complexes with methyl groups (**1** and **3**) showed higher activity than those with the corresponding isopropyl groups (**2** and **5**) but gave lower molecular weight. The higher molecular weight of the polymers and the lower number of polymer chains (N) obtained by **2** and **5** suggest that the *ortho*-isopropyl should suppress chain-transfer reactions.

Leone[7f] et al. reported the polymerization of 1-octene to afford semicrystalline, branched poly(ethylene)-like materials with high molecular weight and narrow molecular weight distribution using a traditional nickel α-dimmine catalyst activated with Et_2AlCl. Recently, we reported that the polymerization of 2-octene[15] and 4-octene[16] with α-diimine nickel catalysts to afford branched polymers with high molecular weight. However, comparison of the effect of linear octene isomers type or polymerization temperature on productivity and polymer structure has not been reported. Herein, we report extension of our studies about the chain-walking polymerization of isomers of linear octane using screened **1**-MMAO under different polymerization conditions.

Polymerization of 1-octene (1O), *trans*-2-octene (2O), 3-octene (3O), and 4O with **1**-MMAO were carried out at various polymerization temperature and time with the [Al]/[Ni] ratio of 500, and the results are listed in Table 2. The catalytic system produced polymers with high molecular weight and narrow molecular weight distribution (M_w/M_n = 1.11−1.72) in moderate yields except 3-octene (entries 10 and 11). We also examined the *trans*-3-hexene using **1**-MMAO under the same conditions, but no polymer was obtained. This result showed that the chain-walking polymerization of 3-octene would not proceed by these α-diimine nickel catalysts. The reason may be attributed to the monomer isomerization of 3-alkene to suppress polymerization. In addition, no polymeric product was obtained from the polymerization of correspond-

DOI: 10.1021/acs.organomet.8b00042
Organometallics 2018, 37, 1358−1367

ing *cis*-isomers of internal octenes using **1**-MMAO under the similar conditions because these *cis*-isomers suppressed the propagation rate.[15]

4O polymerization was conducted at temperatures ranging from −25 to 75 °C (entries 1−5, Table 2), and the results indicated that the highest activity was observed at 25 °C (entry 3). Besides, the increased temperature also affected the molecular weight and its distribution of the produced polymers. Both the highest molecular weight and the narrowest molecular weight distribution (entry 2, M_n = 53.8 kg mol^{-1}, M_w/M_n = 1.19, Table 2) were observed at 0 °C. Further increase of temperature caused a decrease in the molecular weight accompanied by broadening the molecular weight distribution.

The time dependence of 4O polymerization was also investigated (entries 2, 3 and 6−9, Table 2). The catalytic activities were well maintained along with prolonged the reaction time, and the M_n value increased with keeping the narrow molecular weight distribution (0 °C, entries 2 and 6−8, Table 2). Thus, the time-dependences of molecular weight and polydispersity indexes in the polymerization of 4-octene were investigated in more detail under the same polymerization conditions. (Table S2, Supporting Information).

The plot of M_n against the monomer conversion for 4O polymerization catalyzed by **1**-MMAO at 0 °C is plotted in Figure 2. The M_n value increased linearly with increasing 4O

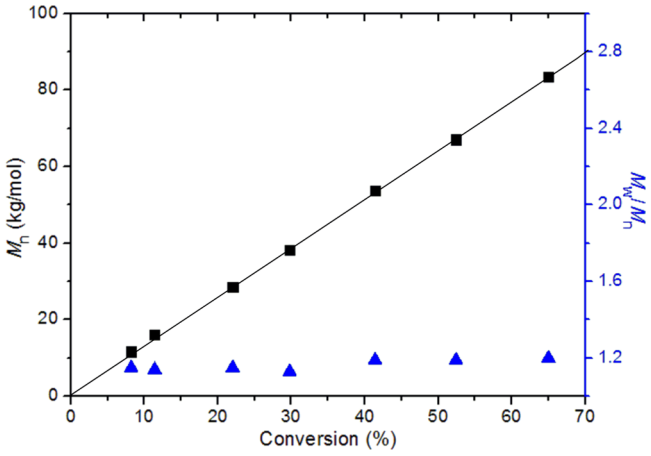

Figure 2. Plots of M_n (■) and M_w/M_n (▲) as a function of monomer conversion for 4-octene polymerization catalyzed by **1**-MMAO at 0 °C.

conversion keeping the narrow molecular weight distribution (M_w/M_n = 1.13−1.20, Figure 2) and the constant number of polymer chains (N). These results verify that the polymerization of 4O with **1**-MMAO proceeded in a living manner at 0 °C within a certain period of time.

Polymerization of 2O was also investigated by **1**-MMAO with the [Al]/[Ni] ratio of 500 at 0 and 25 °C for 2 h (entries 12 and 13, Table 2). These results demonstrated that 2O polymerized slower than 4O. This result may be attributed to the isomerization reaction of 2O to 1O indicated by the lower branching numbers, 121 and 119 per 1000C.[13] The number of branches in the poly(4O), 125/1000C implies that monomer isomerization did not occur in the 4O polymerization, which is discussed in the subsequent section. For comparison, 1O polymerization was performed (entries 14 and 15, Table 2). The catalytic activities decreased in the following order: 1O > 4O ≥ 2O ≫ 3O (0 °C, entries 2, 10, 12, and 14, Table 2). The molecular weight also follows the same trend. The catalytic performances could not be explained with the sole factor of either monomer structure or monomer-isomerization[15] influences, but likely were caused by a combination of both monomer structure and monomer-isomerization effects.

Copolymerization of Linear Octene Isomers. We continued our investigation on the copolymerization of 1O with 2O, 3O, and 4O catalyzed by *para*-phenyl-substituted complexes **1** and **2** activated by MMAO at 0 and 25 °C with the [Al]/[Ni] ratio of 500 and an equal comonomer feed ratio. The copolymerization results are listed in Table 3.

In comparison with homopolymerization of 2O, 3O, and 4O under the same conditions (Table 2), the copolymerization proceeded in high activity. The yields and the molecular weight of the copolymers show the similar trend to those of the homopolymers. For example, the 1O-4O copolymer obtained with **1**-MMAO at 0 °C showed narrow molecular weight distribution (M_w/M_n = 1.13, entry 1, Table 3). Complex **1** bearing two *ortho*-methyl groups showed higher activity than the corresponding isopropyl groups **2** (entries 2 vs 3, Table 3), but gave the copolymer with lower molecular weight. The rates of copolymerization by **1**-MMAO decreased in the following order: 1O-4O > 1O-2O > 1O-3O (entries 2, 4, and 5, Table 3). The molecular weights of the copolymers also follow the same trend.

Structure of the Resulting Polymers. A series of linear octene isomers were successfully polymerized with the α-diimine nickel catalysts activated by MMAO. The total branching degrees of the polymers was determined by ^{1}H NMR spectroscopy, and the results are shown in Tables 1 and 2. The total branching degree of the obtained poly(4O)s was equal to the expected value (125/1000 C) and independent of the [Al]/[Ni] ratio, polymerization temperature, and the catalyst structure. It is known that the total branching degree of the obtained poly(1O)s is lower than the expected value

Table 3. Copolymerization of 1O with 2O, 3O, 4O by Nickel Complexes 1 and 2 Activated by MMAO[a]

	monomers									
entry	1O	M	complex	temp (°C)	yield (mg)	activity[b]	M_n[c] (kg mol^{-1})	M_w/M_n[c]	N[d] (μmol)	branches[e] /1000 C
1	1O	4O	**1**	0	308	15.4	85.9	1.13	3.58	98
2	1O	4O	**1**	25	419	21.0	92.7	1.20	4.52	110
3	1O	4O	**2**	25	401	20.0	107.5	1.21	3.73	106
4	1O	3O	**1**	25	235	11.8	34.7	1.64	6.77	99
5	1O	2O	**1**	25	302	15.1	64.0	1.08	4.72	103

[a]Polymerization conditions: Ni = 10 μmol; cocatalyst MMAO, [Al]/[Ni] = 500; 0.25 g of 1O, 0.25 g of M; polymerization time, 2 h; solvent, toluene; total volume, 5 mL. [b]In unit of kg (mol Ni·h)$^{-1}$. [c]Determined by GPC relative to polystyrene standards. [d]Number of polymer chains calculated by yield and M_n. [e]Branching numbers per 1000 carbon atoms were determined by ^{1}H NMR spectroscopy.

DOI: 10.1021/acs.organomet.8b00042
Organometallics 2018, 37, 1358−1367

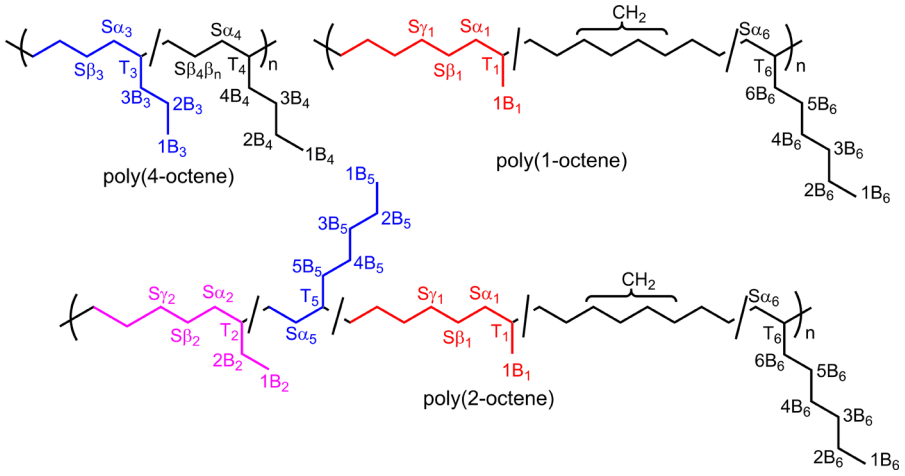

Figure 3. Possible inserted monomer units and their peak assignments of ^{13}CNMR spectra shown in Figure 4. Note on labels: In the denotation of aB_n, the subscript n indicates the branch type (n = 1, 2, 5 or 6). The Arabic number "a" indicates the position from the methyl group of the side chain. The methylene carbons in main chain are labeled by S with two Greek letters followed by an Arabic number which indicate the position from the neighboring methine carbon: for example, $S\alpha_m\beta_n$ indicates the methylene carbon at α position from B_m branch and β position from B_n branch and δ implies the branched carbon at or beyond δ position. The methine carbons are labeled with T_n where n indicates the number of carbons in the branch.

Table 4. Branching Distributions of Poly(4O), Poly(2O), and Poly(1O)

					CH_3/1000 C[a]							
entry/table	complex	nO in poly(nO)	temp (°C)	total CH_3[a]	Me	Et	Pr	Bu	Amy[d]	He	(n+2),8-[b] enchain. (%)	T_g[c] (°C)
4/Table 1	**2**	4O	RT	125			87	38			69.6 (4,8-)	-
7/Table 1	**5**	4O	RT	125			90	35			72.0 (4,8-)	-
1/Table 2	**1**	4O	−25	125			109	16			87.2 (4,8-)	−64.4
2/Table 2	**1**	4O	0	125			102	23			81.3 (4,8-)	−64.7
3/Table 2	**1**	4O	25	125			89	36			70.9 (4,8-)	−65.5
4/Table 2	**1**	4O	50	125			68	57			54.1 (4,8-)	−68.3
5/Table 2	**1**	4O	75	125			64	61			51.2 (4,8-)	−68.9
12/Table 2	**1**	2O	0	117	54	20			37	6	43.2 (2,8-)	−66.5
13/Table 2	**1**	2O	25	116	58	23			26	9	46.4 (2,8-)	−70.0
14/Table 2	**1**	1O	0	95	20		1			74	36.1 (1,8-)	−38.9
15/Table 2	**1**	1O	25	80	39					41	44.8 (1,8-)	−51.5

[a]Branching numbers per 1000 carbon atoms were determined by ^{13}C NMR spectroscopy. [b](n+2),8-Enchainment (n = −1, 0 and 2) was calculated by the following equation: (n+2),8-% = $[C_{n+1}] \times 100$, such as 4,8- = 1,5- = $[C_3]$ = [Pr];[16] 2,8- = $[C_1]$ = [Me];[15] 1,8- = $[C_0]$ = [1000−6B]/(1000 + 2B),[14] B = is the total branching. [c]Determined by DSC. [d]Amy is the abbreviation for amyl.

because the 2,1-insertion of 1O always results in 1,8-enchainment.[13] Actually, the total branching degree of the poly(1O)s obtained at 0 °C was 100/1000 C and decreased to 86/1000 C by raising the polymerization temperature to 25 °C. However, the total branching degree of the obtained poly(2O)s (119−121/1000 C) were slightly less than the expected value (entries 12 and 13, Table 2). The isomerization of 2-octene to 1-octene which forms 1,8-enchainment via 2,1-insertion should be the reason for the lower branch number.

The branching structures of the homopolyoctenes were determined by ^{13}C NMR spectroscopy on the basis of previous work.[7e,15,16,19] The ^{13}CNMR spectra displayed in Figure 3 showed various peaks depending on the monomer, which can be assigned to each monomer-inserted unit as described below, and their contents are summarized in Table 4.

Figure 4 (i) shows the ^{13}C NMR spectrum of the poly(4O)[16] obtained by **2**-MMAO at 20 °C (entry 4, Table 1), which exhibits only propyl (14.76 ppm, $1B_3$; 20.01 ppm, $2B_3$; 36.29 ppm, $3B_3$ and 37.55 ppm, T_3) and butyl (14.38 ppm, $1B_4$; 23.37 ppm, $2B_4$; 29.14 ppm, $3B_4$; 33.55 ppm, $4B_4$ and 37.56 ppm, T_4) branches.

Generally, polymerization temperature has a significant influence on insertion fashion of monomer and chain-walking, thus leading to the change of polymer microstructure.[1d,7] The ^{13}C NMR spectra of the poly(4O)s obtained by **1**-MMAO at polymerization temperatures from −25 to 75 °C are shown in Figure 5. The results showed that the branch structures significantly depended on the polymerization temperature: butyl branch gradually increased as the temperature raised (entries 1−5/Table 2, Table 4) accompanied by the decrease of propyl branch keeping the total branching density constant (125/1000C) as shown in Figure 6. This is consistent with the *ortho-sec*-phenethyl substituted α-diimine nickel initiator.[16] Interestingly, the predominance of propyl branch at low temperature disappeared at 75 °C.

The ^{13}C NMR spectrum of the poly(2O)[15] (Figure 4 (ii)) confirms the presence of methyl (19.92 ppm, $1B_1$), ethyl (11.08 ppm, $1B_2$), amyl (32.60 ppm, $3B_5$), hexyl (31.99 ppm, $3B_6$) branches and a small amount of the long methylene sequence (29.95 ppm, CH_2) derived from 1O formed by monomer-isomerization, whereas that of poly(1O) (Figure 4 (iii)) showed the resonances of methyl (19.76 ppm, $1B_1$) and

DOI: 10.1021/acs.organomet.8b00042
Organometallics 2018, 37, 1358−1367

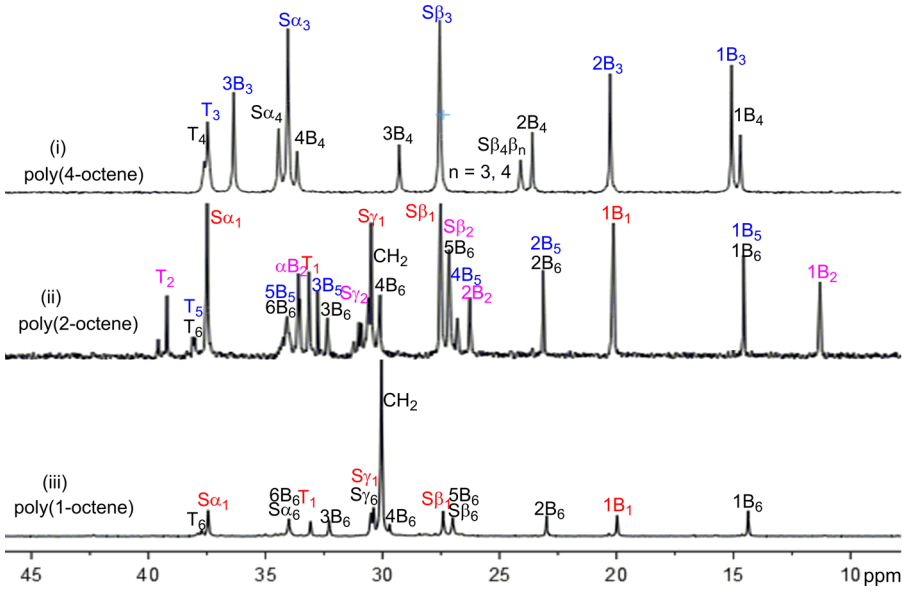

Figure 4. ^{13}C NMR spectra of (i) poly(4O) (entry 4, Table 1), (ii) poly(2O) (entry 13, Table 2), and (iii) poly(1O) (entry 15, Table 2).

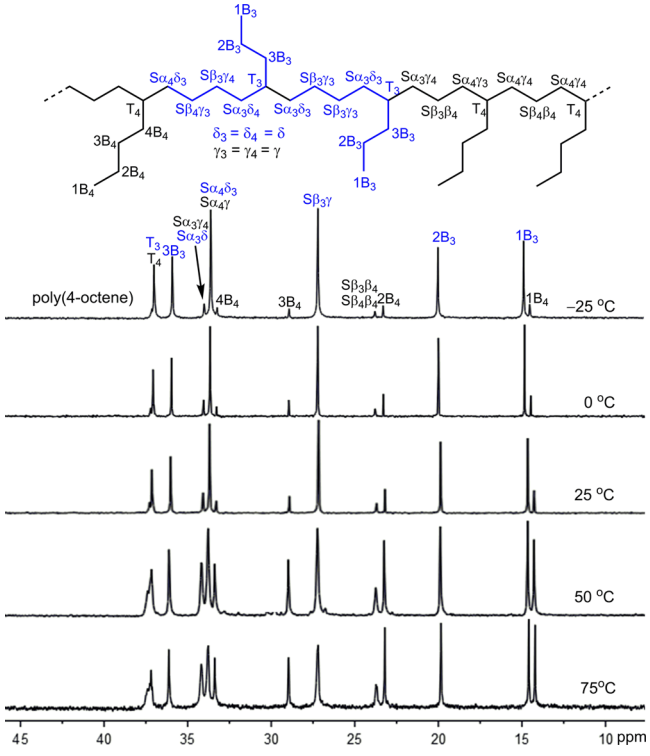

Figure 5. ^{13}C NMR spectra of the poly(4O)s prepared by **1**-MMAO at different polymerization temperatures (entries 1−5, Table 2).

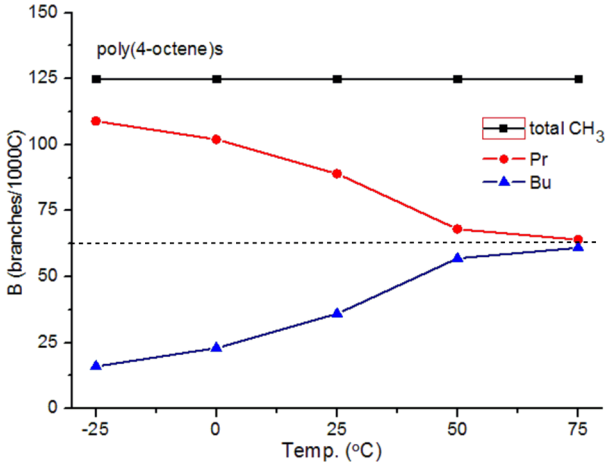

Figure 6. Total branching densities (■) and the branch (Pr:● /Bu:▲) structures of the poly(4O)s versus polymerization temperature at −25, 0, 25, 50, and 75 °C (entries 1−5/Table 2, Table 4).

hexyl (14.18 ppm, $1B_6$) and the long methylene sequence (29.80 ppm, CH_2) due to chain-straightening.

The branching structure of the octene copolymers produced by **1**-MMAO is singled out and analyzed to study the relationship between polymer microstructure and chain-walking mechanism. The branching numbers of the copolymers were decreased in the following order: poly(1O-*co*-4O) > poly(1O-*co*-2O) > poly(1O-*co*-3O) (entries 2, 4 and 5, Table 3). The results can be explained by the relative reactivity of the comonomer to 1O and the probability of comonomer isomerization.

The ^{13}C NMR spectrum of poly(1O-*co*-4O) obtained at 25 °C is shown in Figure 7 (i), which indicates the presence of methyl, propyl, butyl, and hexyl branches.[7e,19] On the assumption that 4O gives either propyl or butyl branch, the comonomer contents and the ratio of 1,8-insertion of 1O can be determined by the following equation (see Table 5).

The branched structure of the poly(1O-*co*-4O) can be safely identified by analyzing Figure 7 (i). The branched 1-octene sequences resulting from catalyst chain-walking, in the presence of methyl (T_1) and hexyl ($2B_6$) branches, are easily detected. At 25 °C, the 4O content in the poly(1O-*co*-4O) produced by **1** is 52 mol % higher than that of 14 mol % at 0 °C (entries 1 and 2, Table 5). The comonomer content in the copolymer depended on the catalyst used, indicating the ligand structure affected the monomer reactivity ratios. For example, the 4O content in the poly(1O-*co*-4O) obtained by complex **1** was slightly higher than that of complex **2** (entries 2 and 3, Table 5) due to the *ortho*-methyl substituted complex **1** shows relatively fast insertion and chain-walking.

DOI: 10.1021/acs.organomet.8b00042
Organometallics 2018, 37, 1358−1367

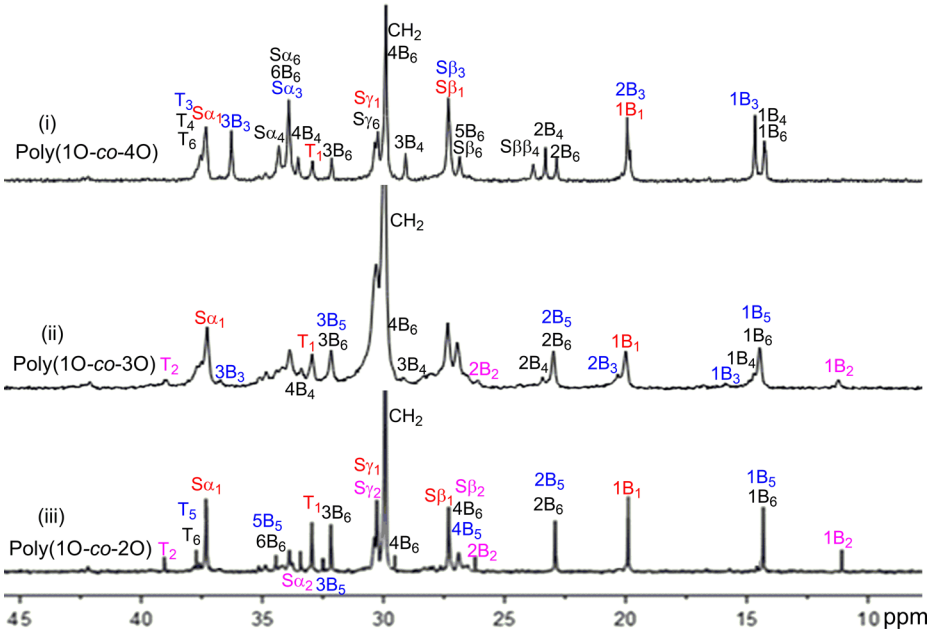

Figure 7. ^{13}C NMR spectra of (i) poly(1O-*co*-4O) (entry 2, Table 3), (ii) poly(1O-*co*-3O) (entry 4, Table 3), and (iii) poly(1O-*co*-2O) (entry 5, Table 3) obtained by **1**-MMAO at 25 °C.

Table 5. Branching Distributions of Octene Copolymers

					CH_3/1000C[a]								
entry	complex	copolymer	temp (°C)	total CH_3[a]	Me	Et	Pr	Bu	Amy	He	1O/M[b] (%)	1,8-En.[c] (%)	T_g[d] (°C)
1	**1**	poly(1O-*co*-4O)	0	100	22		12	5		61	86/14	20.0	−60.6
2	**1**	poly(1O-*co*-4O)	25	108	21		41	24		22	48/52	13.6	−61.6
3	**2**	poly(1O-*co*-4O)	25	105	33		25	30		17	56/44	16.0	−64.6
4	**1**	poly(1O-*co*-3O)	25	98	45	3	1	2	47		n.d.[e]	21.6	−47.9
5	**1**	poly(1O-*co*-2O)	25	102	46	10			4	42	n.d.[e]	18.4	−54.2

[a]Branching numbers per 1000 carbon atoms were determined by ^{13}C NMR spectroscopy. [b][1O]/[4O]-Contents of copolymer was calculated by the following equation: [4O] = [Pr] + [Bu]; [1O] = 1 − [4O]; [c]1,8-Enchainment was calculated by the following equation: 1,8- = [C_0] = [1000−6B]/(1000 + 2B), B = is the total branching. [d]Determined by DSC. [e]Not determined.

The ^{13}C NMR spectra of poly(1O-*co*-3O) and poly(1O-*co*-2O) are also shown in Figure 7 (ii) and (iii), respectively. A small amount of the ethyl branches from 3O and 2O branched units can be detected in the ^{13}C NMR spectra of the poly(1O-*co*-3O) and poly(1O-*co*-2O) (entries 4 and 5, Table 3).[19] However, the 3O content of the poly(1O-*co*-3O) could not be determined because the peak of the amyl branch that was overlapping with that of the hexyl branch (Figure 7 (ii)). The 2O content of the poly(1O-*co*-2O) could also not be determined because of the methyl and hexyl branches from 1O and 2O branched units.

The poly(2O) and poly(4O) obtained had low T_g of approximately −70 ∼ −64 °C (Table 4) and no melting points (T_m), indicating that the polymers were amorphous.[7b] The T_g values were slightly decreased with increasing the polymerization temperature from −25 to 75 °C. The T_g values of the poly(2O) and poly(4O) were almost the same, which were lower than those of the poly(1O)s. The T_g values of the 1O-2O, 1O-3O, and 1O-4O copolymers (Table 5) are higher than that of the 2O, 3O, and 4O polymers, which were also lower than those of the poly(1O).

Polymerization Mechanism of Linear Octenes. Chain-walking alkene polymerization with α-diimine nickel and palladium catalysts affords polymers with unique microstructures.[8] The rate of chain-walking is generally much greater than the rate of alkene insertion.[1e] The poly(4O)s obtained possessed the propyl and butyl branches, of which contents were equal to the amount of monomer units (125/1000 C), while the total branching degree of the poly(2O)s obtained was lower than 125/1000C due to the monomer-isomerization to 1O. The number and the distribution of branches in the poly(octene)s obtained in this study can be explained by the mechanism outlined in Scheme 3.

Linear internal octenes, [$CH_3(CH_2)_nCH{=}CH(CH_2)_mCH_3$, n = 0, 1, and 2], are inserted into Ni−polymer bond via (n+2), (n+3)- or (n+3),(n+2)-insertion. The successive alkene cannot be inserted into the propagation chain of secondary carbons. After the propagation chain-end becomes the methylene carbon via chain-walking, next monomer insertion occurs. If the chain walks to the C1 carbon, the C_{m+1} and C_{m+2} branches are formed in 1,(n+3)- and 1,(n+2)-enchainment ((1) and (4)), respectively. If the chain walks to the opposite direction (C8 carbon), the C_{n+1} and C_{n+2} branches are formed in (n+2), 8- and (n+3), 8-enchainment ((3) and (2)), respectively.

Thus, the linear octenes give the polymers with C_{n+1}, C_{n+2}, C_{m+1}, and C_{m+2} branches. For example, the methyl (C_1), hexyl (C_6) groups and the long methylene sequence (C_0 branch) are detected in the poly(1-octene) (n = −1, m = 5), where 2,1-insertion always gives a long methylene sequence (C_0 branch) in a 1,8-enchainment (3) because of no 1,1-enchainment (4).

DOI: 10.1021/acs.organomet.8b00042
Organometallics 2018, 37, 1358−1367

Scheme 3. Chain-Branching Formation in Linear Octenes Polymerization with α-Diimine Nickel Catalysts

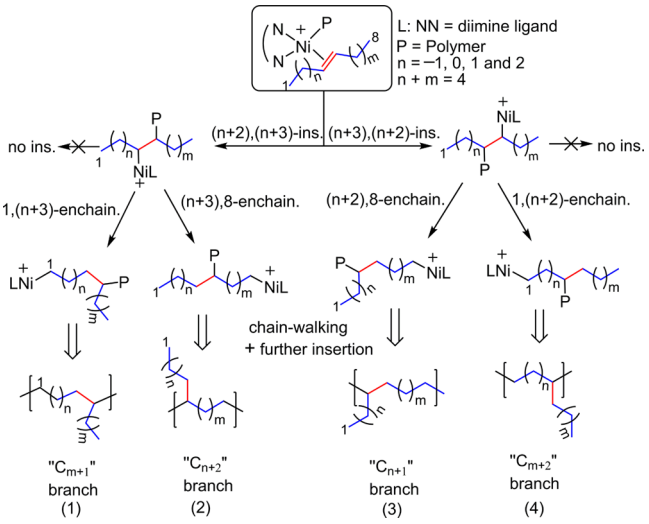

The 2,3- and 3,2-insertion of 2O give four types of branches (i.e., methyl, ethyl, amyl, and hexyl groups). The 4,5- or 5,4-insertion of 4O always give two types of the propyl and butyl groups because of its symmetrical structure. The intensity of the peaks indicated that the propyl sequence ((1) and (3)) is favorable in the poly(4O), because the chain-walking through tert-carbon should be harder than that through the secondary carbon.

Microstructure analysis of the linear octenes polymers (Table 4) indicated that the prioritization of structure units was decreased in the following order, (3) > (1) ≈ (2) > (4) ≫ (5). For example, the structure units of the poly(2O) at 25 °C decreased in the following order, Me (3) > Amy (1) ≈ Et (2) > He (4) ≥ C_0 (5), and those of the poly(4O), Pr (3)/(1) > Bu (2)/(4). In addition, the intensity of the peaks also indicated that the structure unit of (4) should be suppressed at low temperature.

On the other hand, we have confirmed that the monomer-isomerization[20] did not occur in the 4O and higher 1-alkene polymerization by α-diimine nickel catalysts. The former may be suppressed at the polymerization temperature ($T \leq 80$ °C), and the relatively fast insertion and chain-walking, resulting in the production of the no isomerized 4-octene polymer. The microstructures of the produced poly(2O)s indicated the presence of a small amount of the long methylene sequence as shown in Figure 4 (ii), and the number of total branches (116–117) is close to the theoretical value (125). Thus, the rate of 2-octene isomerization is much lower than the rate of its insertion.

CONCLUSIONS

In summary, we reported the polymerization of internal alkenes, i.e., *trans*-2-, *trans*-3-, and *trans*-4-octene using the screened α-diimine nickel catalysts containing phenyl groups upon activation with MMAO in comparison with the 1-octene polymerization. The results indicated that 2- and 4-octenes underwent chain-walking polymerization to give new materials of up to 83.4 kg mol^{-1} and narrow M_w/M_n values (<2.0). However, 3-octene was not polymerized by this nickel catalytic system. The rates of polymerization were found to decrease in the following order: 1-octene > 4-octene ≥ 2-octene ≫ 3-octene. At 0 °C, 4-octene polymerized in a living/controlled manner. The NMR analyses of the polymers showed that 4-octene was achieved by chain-walking polymerization to give periodically branched polymers with the constant branching density, while the total branching degree of the obtained poly(2-octene)s are less than the expected value due to monomer isomerization.

Based on chain-walking polymerization mechanism studies of linear internal octenes, the general formula of chain-branching formation of linear alkene was provided to indicate the direction for the design of new catalysts. The (*n*+2),(*n*+3)- and (*n*+3),(*n*+2)-insertion of the internal (*n*+2)-alkene [$CH_3(CH_2)_nCH{=}CH(CH_2)_mCH_3$], chain-walking, and insertion at certain points along the chain was confirmed by the ^{13}C NMR analysis of the produced polymers with various types of branches including C_{n+1}, C_{n+2}, C_{m+1}, and C_{m+2} branches. The obtained internal octene polymers are amorphous elastomers with low T_g of approximately −66 °C. The branching structure depended on the polymerization temperature. Interestingly, **1** was found to polymerize *trans*-4-octene with high levels of 1,5-regioselectivity at −25 °C (up to 87.2%). At 75 °C, the number of propyl and butyl branches became almost equal. Additionally, copolymerization of 1-octene and these linear octene isomers were studied by *para*-phenyl-substituted complexes with equal comonomer feed ratio. These copolymerization showed higher activities than the 2-, 3-, and 4-octene homopolymerization, and the molecular weight of the copolymers showed the similar trend to those of the homopolymers.

EXPERIMENTAL SECTION

General Considerations. All manipulations were performed under nitrogen gas using standard Schlenk techniques. Modified methylaluminoxane (MMAO, 6.5 wt % Al, 2.17 M in toluene) was donated by Tosoh-Finechem Co. Dichloromethane was distilled from CaH_2 under dry nitrogen. Toluene and 1,2-dimethoxyethane (DME) were distilled from sodium/benzophenone under nitrogen atmosphere and distilled before use. 1-, *trans*-2-, *trans*-3-, and *trans*-4-octenes were purchased from TCI Chemical Co., and these monomers were dried over 4 Å molecular sieves overnight and degassed under nitrogen flow before use. Nickel complexes **1**,[13] **3**,[13] **5**,[16] and **6**[16] were synthesized according to the literature. Other chemicals were commercially obtained and purified with common procedures.

^1H and ^{13}C NMR spectra of compounds and polymers were recorded on a Varian 400 MHz NMR instrument at room temperature and 50 °C, respectively, using $CDCl_3$ as a solvent and tetramethylsilane (TMS) as a reference for the compounds. The peak of the solvent (^{13}C: 77.16 ppm) was used as an internal reference in ^{13}C NMR spectra of the polymers. X-ray diffraction data were collected at 298(2) K on a Bruker Smart CCD area detector with graphite-monochromated Mo Kα radiation (λ = 0.71073 Å). IR spectra were recorded on a JASCO FT/IR-300E spectrophotometer on KBr pellets. Elemental analysis was carried out using a PerkinElmer 2400 Series II. Number-average molecular weight (M_n) and molecular weight distribution (M_w/M_n) of the polymers were determined by a Tosoh HLC-8320GPC chromatograph at 40 °C using tetrahydrofuran (THF) as an eluent and calibrated with polystyrene standard. DSC analysis of the polymers was performed by a SII EXSTAR6000 system.

Synthesis of Complexes 2 and 4. *Synthesis of Bis[N,N′-(2,6-diisopropyl-4-phenylphenyl)imino]acenaphthene (**L2**).* Formic acid (0.2 mL) was added to a stirred solution of 1,2-acenaphthylenedione (0.091 g, 0.50 mmol) and 2,6-diisopropyl-4-phenylaniline (0.27 g, 1.05 mmol) in MeOH (30 mL). The mixture was refluxed for 12 h, then cooled and the precipitate was separated by filtration. The solid was recrystallized from MeOH/CH_2Cl_2 (v/v = 15:1), washed with cold ethanol, and dried under vacuum (0.24 g, 74% yield). ^1H NMR (400

DOI: 10.1021/acs.organomet.8b00042
Organometallics 2018, 37, 1358–1367

MHz, $CDCl_3$): δ 7.89 (d, J = 8.0 Hz, 2H, Nap−H), 7.71−7.76 (m, 4H, Nap−H and Ar−H), 7.48−7.54 (m, 8H, Ar−H), 7.35 (dd, J = 7.6 Hz, 4H, Ar−H), 6.78 (d, J = 7.6 Hz, 2H, Nap−H), 3.07−3.13 (m, 4H, $-CH(CH_3)_2$), 1.29 (d, J = 7.8 Hz, 12H, $-CH_3$), 1.04 (d, J = 7.8 Hz, 12H, $-CH_3$). ^{13}C NMR (100 MHz, $CDCl_3$): δ 161.09 (C═N), 146.95, 141.70, 140.82 (Nap−C), 136.87, 135.84, 131.11, 129.45(Nap−C), 128.99, 128.74 (Nap−C), 127.93, 126.87, 126.80, 123.43, 122.30 (Nap−C), 28.77 ($-CH(CH_3)_3$), 23.19 ($-CH_3$). Anal. Calcd for $C_{48}H_{48}N_2$: C, 88.30; H, 7.41; N, 4.29. Found: C, 88.19; H, 7.38; N, 4.23. FT-IR (KBr): 1652 cm^{-1} ($\nu_{C=N}$).

Synthesis of Bis[N,N′-(2-methy-6-isopropylphenyl)imino]-acenaphthene (L4). Using the same synthetic procedure for **L2**, **L4** was obtained as an orange-red powder (0.19 g, 89% yield). ^1H NMR (400 MHz, $CDCl_3$): δ 7.88 (d, J = 8.0 Hz, 2H, Nap−H), 7.36 (t, J = 7.8 Hz, 2H, Nap−H), 7.26 (dd, J = 7.2 Hz, 2H, Ar−H), 7.14−7.17 (m, 4H, Ar−H), 6.67 (d, J = 7.2 Hz, 2H, Nap−H), 3.03−3.07 (m, 2H, $-CH(CH_3)_2$), 2.11 (s, 12H, $-CH_3$), 1.24 (d, J = 6.8 Hz, 6H, $-CH(CH_3)_2$), 0.95 (d, J = 6.8 Hz, 6H, $-CH(CH_3)_2$). ^{13}C NMR (100 MHz, $CDCl_3$): δ 161.10, 148.09, 140.72, 136.00, 132.61, 131.03, 129.40, 128.97, 128.12, 124.15, 123.68, 122.89, 28.63 ($-CH(CH_3)_3$), 23.71 ($-CH(CH_3)_3$, 22.69 ($-CH(CH_3)_3$, 18.85 ($-CH_3$). Anal. Calcd for $C_{32}H_{32}N_2$: C, 86.44; H, 7.25; N, 6.30. Found: C, 86.37; H, 7.31; N, 6.21. FT-IR (KBr): 1633 cm^{-1} ($\nu_{C=N}$).

Synthesis of {Bis[N,N′-(2,6-diisopropyl-4-phenylphenyl)imino]-acenaphthene}dibromonickel (2). [(DME)$NiBr_2$] (0.16 g, 0.50 mmol) and **L2** (0.37 g, 0.50 mmol) were combined in a Schlenk flask under a N_2 atmosphere. CH_2Cl_2 (20 mL) was added, and the reaction mixture was stirred at room temperature for 24 h. The resulting suspension was filtered. The solvent was removed under vacuum and the residue was washed with diethyl ether (3 × 15 mL), and then dried under vacuum at room temperature to give nickel complex **2** (0.38 g, 87% yield). Anal. Calcd for $C_{48}H_{48}Br_2N_2Ni$: C, 66.16; H, 5.55; N, 3.21. Found: C, 66.23; H, 5.50; N, 3.17. FT-IR (KBr) 1650 cm^{-1} ($\nu_{C=N}$).

Synthesis of {Bis[N,N′-(2-methy-6-isopropylphenyl)imino]-acenaphthene}dibromonickel (4). Using the same synthetic procedure for **2**, **4** was obtained as a dark-red powder (0.31 g, 93% yield). Anal. Calcd for $C_{32}H_{32}Br_2N_2Ni$: C, 57.96; H, 4.86; N, 4.22. Found: C, 57.91; H, 4.79; N, 4.28. FT-IR (KBr) 1642 cm^{-1} ($\nu_{C=N}$).

X-ray Structure Determinations. A single crystal of complex **2** suitable for X-ray analysis was obtained by dissolving the nickel complex in CH_2Cl_2, followed by slow layering of the resulting solution with *n*-hexane at room temperature. Data collections were performed at 296(2) K on a Bruker SMART APEX diffractometer with a CCD area detector, using graphite monochromated Mo Kα radiation (λ = 0.71073 Å). The determination of crystal class and unit cell parameters was carried out by the SMART program package. The raw frame data were processed using SAINT and SADABS to yield the reflection data file. The structures were solved by using the SHELXTL program. Refinement was performed on F^2 anisotropically for all non-hydrogen atoms by the full-matrix least-squares method. The hydrogen atoms were placed at the calculated positions and were included in the structure calculation without further refinement of the parameters. Details of the crystal data and structure refinements for complex **2** are listed in Table S1.

Procedure for Polymerization of Octenes. Polymerization of octene was carried out in a 10-mL glass reactor equipped with a magnetic stirrer. After drying the reactor under N_2 atmosphere, toluene was added to the reactor. Octene was added to the toluene kept at polymerization temperature via a syringe. Then the co-catalyst MMAO was added to the toluene and the mixture was stirred for 10 min. Polymerization was started by the addition of the catalyst solution in toluene. Polymerization was terminated with 100 mL of a 3% HCl−MeOH solution. The polymers obtained were adequately washed with methanol and dried under vacuum at 60 °C for 3 h.

■ ASSOCIATED CONTENT

Supporting Information

The Supporting Information is available free of charge on the ACS Publications website at DOI: 10.1021/acs.organomet.8b00042.

NMR spectra of compounds (Figures S1−S8) and (co)polymers (Figures S12−S23); GPC and DSC curves of polymers samples (Figures S11 and S24−S37); figures, tables, and CIF files giving crystallographic data (PDF)

Accession Codes

CCDC 979238 contains the supplementary crystallographic data for this paper. These data can be obtained free of charge via www.ccdc.cam.ac.uk/data_request/cif, or by emailing data_request@ccdc.cam.ac.uk, or by contacting The Cambridge Crystallographic Data Centre, 12 Union Road, Cambridge CB2 1EZ, UK; fax: +44 1223 336033.

■ AUTHOR INFORMATION

Corresponding Authors

*E-mail for F.W: wangfuzhou1718@126.com.
*E-mail for T.S: tshiono@hiroshima-u.ac.jp.

ORCID

Fuzhou Wang: 0000-0003-0470-7110
Ryo Tanaka: 0000-0002-6085-074X
Takeshi Shiono: 0000-0002-1118-9991

Notes

The authors declare no competing financial interest.

■ ACKNOWLEDGMENTS

The authors are grateful to Tosoh-Finechem Co., Ltd. for the generous donation of MMAO. The NMR measurements were made at the Natural Science Center for Basic Research and Development (N-BARD), Hiroshima University.

■ REFERENCES

(1) (a) Domski, G. J.; Rose, J. M.; Coates, G. W.; Bolig, A. D.; Brookhart, M. *Prog. Polym. Sci.* **2007**, *32*, 30−92. (b) Nakamura, A.; Ito, S.; Nozaki, K. *Chem. Rev.* **2009**, *109*, 5215−5244. (c) Bianchini, C.; Giambastiani, G.; Luconi, L.; Meli, A. *Coord. Chem. Rev.* **2010**, *254*, 431−455. (d) Chen, M.; Yang, B. P.; Chen, C. L. *Angew. Chem., Int. Ed.* **2015**, *54*, 15520. (e) Guo, L. H.; Dai, S. Y.; Sui, X. L.; Chen, C. L. *ACS Catal.* **2016**, *6*, 428−441. (f) Long, B. K.; Eagan, J. M.; Mulzer, M.; Coates, G. W. *Angew. Chem.* **2016**, *128*, 7222−7226. (g) Guo, L. H.; Liu, W.; Chen, C. L. *Mater. Chem. Front.* **2017**, *1*, 2487−2494. (h) Chen, M.; Chen, C. L. *ACS Catal.* **2017**, *7*, 1308−1312. (i) Yasuda, H.; Nakano, R.; Ito, S.; Nozaki, K. *J. Am. Chem. Soc.* **2018**, *140*, 1876−1883. (j) Chen, M.; Chen, C. L. *Angew. Chem., Int. Ed.* **2018**, *57*, 3094−3098.

(2) (a) Ittel, S. D.; Johnson, L. K.; Brookhart, M. *Chem. Rev.* **2000**, *100*, 1169−1203. (b) Chen, G.; Ma, X. S.; Guan, Z. *J. Am. Chem. Soc.* **2003**, *125*, 6697−6704. (c) Chen, C.; Luo, S.; Jordan, R. F. *J. Am. Chem. Soc.* **2008**, *130*, 12892−12893. (d) Chen, E. Y. X. *Chem. Rev.* **2009**, *109*, 5157−5214. (e) Chen, C.; Jordan, R. F. *J. Am. Chem. Soc.* **2010**, *132*, 10254−10255. (f) Chen, C.; Luo, S. J.; Jordan, R. F. *J. Am. Chem. Soc.* **2010**, *132*, 5273−5284. (g) Guo, L. H.; Dai, S. Y.; Chen, C. L. *Polymers* **2016**, *8*, 37. (h) Fu, X.; Zhang, L. J.; Tanaka, R.; Shiono, T.; Cai, Z. G. *Macromolecules* **2017**, *50*, 9216−9221. (i) Zou, C.; Dai, S. Y.; Chen, C. L. *Macromolecules* **2018**, *51*, 49−56.

(3) (a) Dong, J. Y.; Hu, Y. *Coord. Chem. Rev.* **2006**, *250*, 47−65. (b) Rhinehart, J. L.; Brown, L. A.; Long, B. K. *J. Am. Chem. Soc.* **2013**, *135*, 16316−16319. (c) Yuan, J. C.; Wang, F. Z.; Xu, W. B.; Mei, T. J.; Li, J.; Yuan, B. N.; Song, F. Y.; Jia, Z. *Organometallics* **2013**, *32*, 3960−

DOI: 10.1021/acs.organomet.8b00042
Organometallics 2018, 37, 1358−1367

3968. (d) Dai, S. Y.; Sui, X. L.; Chen, C. L. *Angew. Chem., Int. Ed.* **2015**, *54*, 9948−9953. (e) Chen, Z.; Liu, W.; Daugulis, O.; Brookhart, M. *J. Am. Chem. Soc.* **2016**, *138*, 16120−16129. (f) Dai, S. Y.; Chen, C. L. *Angew. Chem., Int. Ed.* **2016**, *55*, 13281−13285. (g) Dai, S. Y.; Zhou, S. X.; Zhang, W.; Chen, C. L. *Macromolecules* **2016**, *49*, 8855−8862. (h) Sui, X. L.; Hong, C. W.; Pang, W. M.; Chen, C. L. *Mater. Chem. Front* **2017**, *1*, 967−972. (i) Chen, Z.; Leatherman, M. D.; Daugulis, O.; Brookhart, M. *J. Am. Chem. Soc.* **2017**, *139*, 16013−16022. (j) Zhou, S. X.; Chen, C. L. *Sci. Bull.* **2018**, *63*, 441−445.

(4) (a) Guan, Z.; Cotts, P. M.; McCord, E. F.; McLain, S. J. *Science* **1999**, *283*, 2059−2062. (b) Okada, M.; Nakayama, Y.; Ikeda, T.; Shiono, T. *Macromol. Rapid Commun.* **2006**, *27*, 1418−1423. (c) Wang, F. Z.; Yuan, J. C.; Song, F. Y.; Li, J.; Jia, Z.; Yuan, B. N. *Appl. Organomet. Chem.* **2013**, *27*, 319−327. (d) Liu, J.; Chen, D. R.; Wu, H.; Xiao, Z. F.; Gao, H. Y.; Zhu, F. M.; Wu, Q. *Macromolecules* **2014**, *47*, 3325−3331. (e) Chen, Z.; Allen, K. E.; White, P. S.; Daugulis, O.; Brookhart, M. *Organometallics* **2016**, *35*, 1756−1760. (f) Zou, W. P.; Chen, C. L. *Organometallics* **2016**, *35*, 1794−1801. (g) Lian, K.; Zhu, Y.; Li, W.; Dai, S. Y.; Chen, C. L. *Macromolecules* **2017**, *50*, 6074−6080. (h) Na, Y. N.; Zhang, D.; Chen, C. L. *Polym. Chem.* **2017**, *8*, 2405−2409.

(5) (a) Cherian, A. E.; Rose, J. W.; Lobkovsky, E. B.; Coates, G. W. *J. Am. Chem. Soc.* **2005**, *127*, 13770−13771. (b) McCord, E. F.; McLain, S. J.; Nelson, L. T. J.; Ittel, S. D.; Tempel, D.; Killian, C. M.; Johnson, L. K.; Brookhart, M. *Macromolecules* **2007**, *40*, 410−420. (c) Hu, H.; Zhang, L.; Gao, H.; Zhu, F.; Wu, Q. *Chem. - Eur. J.* **2014**, *20*, 3225−3233. (d) Guo, L. H.; Chen, C. L. *Sci. China: Chem.* **2015**, *58*, 1663−1673. (e) Wang, R. K.; Sui, X. L.; Pang, W. M.; Chen, C. L. *ChemCatChem* **2016**, *8*, 434−440. (f) Zhao, M. H.; Chen, C. L. *ACS Catal.* **2017**, *7*, 7490−7494. (g) Zhai, F.; Jordan, R. F. *Organometallics* **2017**, *36*, 2784−2799.

(6) (a) Ye, Z.; Alsyouri, H.; Zhu, S.; Lin, Y. S. *Polymer* **2003**, *44*, 969−980. (b) Carrow, B. P.; Nozaki, K. *Macromolecules* **2014**, *47*, 2541−2555. (c) Liu, J.; Chen, D. R.; Wu, H.; Xiao, Z. F.; Gao, H. Y.; Zhu, F. M.; Wu, Q. *Macromolecules* **2014**, *47*, 3325−3331. (d) Hu, H.; Gao, H.; Chen, D.; Li, G.; Tan, Y.; Liang, G.; Zhu, F.; Wu, Q. *ACS Catal.* **2015**, *5*, 122−128. (e) Li, M.; Wang, X. B.; Luo, Y.; Chen, C. L. *Angew. Chem., Int. Ed.* **2017**, *56*, 11604−11609.

(7) (a) Camacho, D. H.; Guan, Z. *Macromolecules* **2005**, *38*, 2544−2546. (b) Vaidya, T.; Klimovica, K.; LaPointe, A. M.; Keresztes, I.; Lobkovsky, E. B.; Daugulis, O.; Coates, G. W. *J. Am. Chem. Soc.* **2014**, *136*, 7213−7216. (c) Takeuchi, D.; Osakada, K. *Polymer* **2016**, *82*, 392−405. (d) Sun, J. L.; Wang, F. Z.; Li, W. M.; Chen, M. *RSC Adv.* **2017**, *7*, 55051−55059. (e) O'Connor, K. S.; Lamb, J. R.; Vaidya, T.; Keresztes, I.; Klimovica, K.; LaPointe, A. M.; Daugulis, O.; Coates, G. W. *Macromolecules* **2017**, *50*, 7010−7027. (f) Leone, G.; Mauri, M.; Pierro, I.; Ricci, G.; Canetti, M.; Bertini, F. *Polymer* **2016**, *100*, 37−44.

(8) (a) Takeuchi, D.; Chiba, Y.; Takano, S.; Osakada, K. *Angew. Chem., Int. Ed.* **2013**, *52*, 12536−12540. (b) Wang, Z.; Liu, Q. B.; Solan, G. A.; Sun, W. H. *Coord. Chem. Rev.* **2017**, *350*, 68−83. (c) Wang, F. Z.; Tian, S. S.; Li, R. P.; Li, W. M.; Chen, C. L. *Chin. J. Polym. Sci.* **2018**, *36*, 157−162.

(9) (a) Jia, D.; Zhang, W.; Liu, W.; Wang, L.; Redshaw, C.; Sun, W. H. *Catal. Sci. Technol.* **2013**, *3*, 2737−2745. (b) Zhong, L.; Li, G.; Liang, G.; Gao, H.; Wu, Q. *Macromolecules* **2017**, *50*, 2675−2682. (c) Rong, C. Y.; Wang, F. Z.; Li, W. M.; Chen, M. *Organometallics* **2017**, *36*, 4458−4464. (d) Rosar, V.; Meduri, A.; Montini, T.; Fornasiero, P.; Zangrando, E.; Milani, B. *Dalton Trans.* **2018**, *47*, 2778−2790.

(10) Dai, S. Y.; Sui, X. L.; Chen, C. L. *Chem. Commun.* **2016**, *52*, 9113−9116.

(11) (a) Leatherman, M. D.; Brookhart, M. *Macromolecules* **2001**, *34*, 2748−2750. (b) Cherian, A. E.; Lobkovsky, E. B.; Coates, G. W. *Chem. Commun.* **2003**, 2566−2567. (c) Liu, W. J.; Brookhart, M. *Organometallics* **2004**, *23*, 6099−6107. (d) Milano, G.; Guerra, G.; Mazzeo, M.; Pellecchia, C.; Cavallo, L. *Macromolecules* **2005**, *38*, 2072−2075. (e) Endo, K.; Kondo, Y. *Polym. J.* **2006**, *38*, 1160−1164.

(12) Endo, K.; Kondo, Y. *J. Polym. Sci., Part A: Polym. Chem.* **2008**, *46*, 2858−2863.

(13) (a) Yuan, J. C.; Wang, F. Z.; Yuan, B. N.; Jia, Z.; Song, F. Y.; Li, J. *J. Mol. Catal. A: Chem.* **2013**, *370*, 132−139. (b) Wang, F. Z.; Yuan, J. C.; Li, Q. S.; Tanaka, R.; Nakayama, Y.; Shiono, T. *Appl. Organomet. Chem.* **2014**, *28*, 477−483. (c) Wang, F. Z.; Tanaka, R.; Li, Q. S.; Yuan, J. C.; Nakayama, Y.; Shiono, T. *J. Mol. Catal. A: Chem.* **2015**, *398*, 231−240. (d) Wang, F. Z.; Li, R. P.; Tian, S. S.; Lian, K. B.; Guo, D. F.; Li, W. M. *Appl. Organomet. Chem.* **2018**, *32*, e4298.

(14) Wang, F. Z.; Tanaka, R.; Cai, Z. G.; Nakayama, Y.; Shiono, T. *Polymers* **2016**, *8*, 160.

(15) Wang, F. Z.; Tanaka, R.; Cai, Z. G.; Nakayama, Y.; Shiono, T. *Polymer* **2017**, *127*, 88−100.

(16) Wang, F. Z.; Tanaka, R.; Cai, Z. G.; Nakayama, Y.; Shiono, T. *Macromol. Rapid Commun.* **2016**, *37*, 1375−1381.

(17) Liu, J. Y.; Li, Y. G.; Li, Y. S.; Hu, N. H. *J. Appl. Polym. Sci.* **2008**, *109*, 700−707.

(18) Ward, L. G. L.; Pipal, J. R. *Inorg. Synth.* **1972**, *13*, 162−163.

(19) (a) McCord, E. F.; McLain, S. J.; Nelson, L. T. J.; Ittel, S. D.; Tempel, D.; Killian, C. M.; Johnson, L. K.; Brookhart, M. *Macromolecules* **2007**, *40*, 410−420. (b) Azoulay, J. D.; Bazan, G. C.; Galland, G. B. *Macromolecules* **2010**, *43*, 2794−2800.

(20) (a) Vasseur, A.; Bruffaerts, J.; Marek, I. *Nat. Chem.* **2016**, *8*, 209−219. (b) Kocen, A. L.; Klimovica, K.; Brookhart, M.; Daugulis, O. *Organometallics* **2017**, *36*, 787−790.

DOI: 10.1021/acs.organomet.8b00042
Organometallics 2018, 37, 1358−1367